Compact spoof surface plasmon polariton waveguide with asymmetric serrations

Cheng An[1], Zhenning Xiao[1], Weiwen Li[1,*] , and Yu Wang[1]

[1]*Department of Electronic Engineering, Xiamen University, Xiamen 361005, China*

ABSTRACT

Spoof surface plasmon polaritons (SSPPs) at microwave band can be implemented on thin conductor layer with periodic patterns. However, the lateral width of SSPP waveguides tends to be large at low frequencies, which is not conducive to device miniaturization. In this paper, a compact SSPP waveguide structure based on asymmetric serration conductor units is proposed to further reduce the transverse size of device. Specifically, the cutoff frequency of this SSPP waveguide is reduced by lengthening the lateral conductor strips at asymmetric serration unit tops. Since the variation range of top strip length is large in this case, the adjustable range of the waveguide passband is increased. For the waveguide prototype with an overall width of 13.0 mm, the cutoff frequency can be effectively regulated in the range of 7.2–11.3 GHz.

1 Introduction

Surface plasmon polaritons (SPPs) formed by the interaction of free electrons and photons travel along the interface between metals and medium, and exhibit near-field enhancement, surface confinement, and deep subwavelength characteristics [1]. At optical frequencies, metals exhibit dielectric characteristics and have negative equivalent dielectric constants. Since metals behave as good conductors in microwave and millimeter wave bands, periodic holes are introduced into the metal interface to reduce the equivalent plasmon resonance frequency [2]. In this case, the slow waves along the interface are similar to optical SPP modes, and are called spoof SPPs (SSPPs) [3–5].

Using SSPP modes, it is possible to achieve thin-layer microwave waveguides or devices and save ground conductors [6, 7]. Due to the strong confinement, the SSPP mode radiation loss is low and its propagation can even be implemented in bent structures [8–11]. Meanwhile, we can control the dispersion characteristics of the SSPP mode by adjusting the structure and size of the periodic unit, to well regulate the operating band of SSPP devices [12–14]. The H-shaped periodic unit is mostly used for SSPP waveguides [15–17]. To enhance the confinement effect of SSPP modes in a lower frequency band, the groove depth h has to be increased, and thus a wider unit structure is necessary, which is not conducive to the miniaturization of SSPP devices [18].

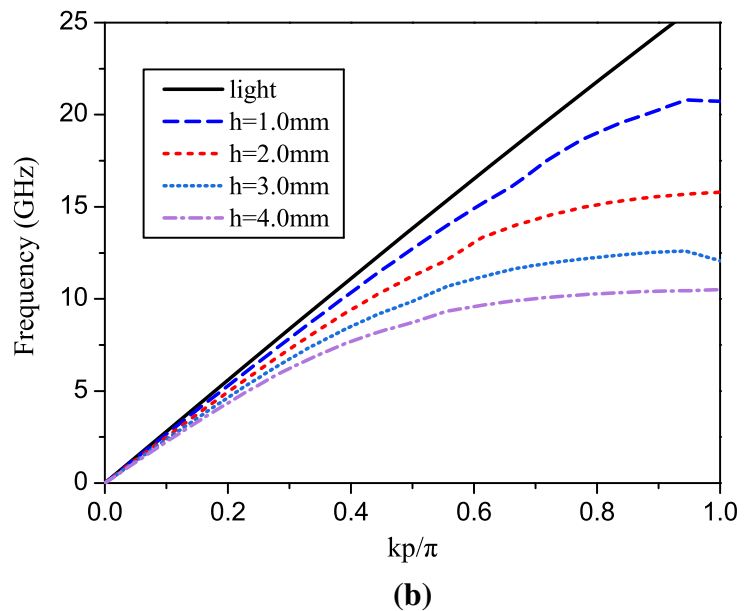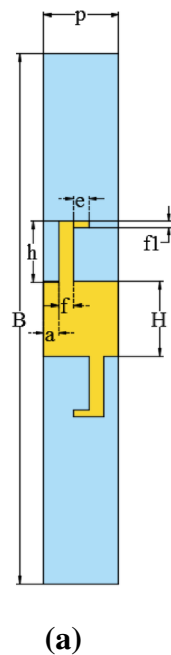In this paper, the H-shaped unit is replaced by asymmetric serration structure. The introduction of

---

Address correspondence to E-mail: wwl@xmu.edu.cn

lateral conductor strips on top of the serration unit improves the ability to constrain surface fields and reduces the cutoff frequency. The structure asymmetry also increases the variable range of the lateral conductor length, so the adjustable feature of the waveguide passband is improved. As a prototype for the SSPP waveguide with a conductor width of 13.0 mm, the cutoff frequency can be regulated in the range from 7.2 to 11.3 GHz by changing the lateral strip length.

2 SSPP waveguide

The proposed periodic unit with asymmetric serrations for the SSPP waveguide is shown in Fig. 1. It is fabricated on a single-layer copper-coated F4BM microwave substrate with a thickness of 0.8 mm, a permittivity of 2.2, and a loss tangent of 0.01. The asymmetric serration unit conductor with the period of $p = 5.0$ mm is laid on the dielectric substrate of the width of $B = 35.8$ mm. The width of the central conductor strip for the unit structure is $H = 5.0$ mm. The width of the vertical strips in the zigzag conductors is $f = 0.8$ mm and its height is marked as h. The distance between the vertical conductor strip and the nearest periodic boundary is $a = 1.0$ mm. The length and width of the top rectangular conductors for the zigzag structures are $e = 1.0$ mm and $f_1 = 0.4$ mm, respectively.

For H-shaped periodic unit, there is the theoretical dispersion: $\sqrt{k^2 - k_0^2}/k_0 = (d/p)\tan(k_0 h).$, where k_0 is the phase constants of plane waves, and d is the slot width of the groove [19–22]. Obviously, the period p and the groove depth h are the main structural parameters affecting the operating band of a SSPP waveguide. For the unit structure shown in Fig. 1a, the groove depth corresponds to the height of the zigzag conductors on both sides. Using eigenmode analysis tool of the electromagnetic software CST Studio Suite, the influence of the height h on the dispersion characteristics is shown in Fig. 1b. It can be seen that as the vertical conductor height h increases, the asymptotic frequency of the dispersion curve decreases. In fact, the plasmon oscillation follows the Lorentz model, and the oscillation frequency is related to the electron concentration and equivalent mass [23]. Periodic grooves increase the electron-equivalent mass, resulting in a decrease in the plasmon oscillation frequency in serration conductors.

However, as the height h continues to increase, this decrease becomes slow. The periodic unit of $h = 4.0$ mm is used to construct the SSPP waveguide. In this case, the asymptotic frequency is 10.6 GHz. As shown in Fig. 2, the SSPP waveguide structure comprises three distinct regions. Region I is the coplanar waveguide (CPW) as feeding ports, region II is the transition part between CPW mode and SSPP mode, and region III is the transmission part of SSPP mode.

Fig. 1 a Schematic diagram of periodic unit with asymmetric serration conductors, and b the corresponding dispersion characteristics, where k is the phase constant and p is the period

(a)

(b)

Regions I and II are partially enlarged as shown in Fig. 2b. To match the sub-miniature-A (SMA) connector with a characteristic impedance of 50 Ω, the width of CPW inner conductor is set to $H = 5.0$ mm, the width of the outer ground conductor is $w = 15.0$ mm, and the gap between inner and outer conductors is $s = 0.4$ mm. The CPW length is $L_1 = 10.0$ mm. Region II includes two 1/4-elliptical ground planes and an intermediate conductor composed of 8 serration units with graded height. The semi-major axis of the ellipse is $L_2 = 50.0$ mm, and the semi-minor axis is $w = 15.0$ mm. The height of the zigzag structures increases uniformly from $h_1 = 0.5$ mm to $h = 4.0$ mm with a step of 0.5 mm, while its lateral conductor length e remains the same. Through the gradual change of the zigzag structure height, the momentum matching between the CPW TEM mode and the SSPP mode can be effectively implemented [24–30]. Finally, the SSPP modes travel in Region III, which consists of 22 identical asymmetric serration units with a total length of 110.0 mm. Including the feeding ports, the whole length of the SSPP waveguide is $A = 230.0$ mm and the width is $B = 35.8$ mm.

According to the structure shown in Fig. 2, a SSPP waveguide prototype with $h = 4.0$ mm and $e = 1.0$ mm is manufactured by etching method. After the two ports are soldered with SMA connectors, its scattering characteristics are tested by a two-port vector network analyzer AV3629D. The simulation is performed using software CST Studio Suite. The simulation and test comparison for the transmission characteristics is shown in Fig. 3. As far as simulation results are considered, the pass band is 0.7–10.1 GHz. The matching performance near the low-frequency end is worse than at the high-frequency side, where has a steep cutoff. The trend of measured data agrees with the simulation results. However, the measured passband is narrowed, which is related to material loss, processing and test errors.

3 Regulation of cutoff frequency

The groove depth h of the periodic structure has the obvious regulation effect on the cutoff frequency of the SSPP waveguide. However, for low cut-off frequency, deep grooves and wide center conductor are required, which is not conducive to device miniaturization. The use of lateral conductor strip in the constructed SSPP structure is essentially a method of
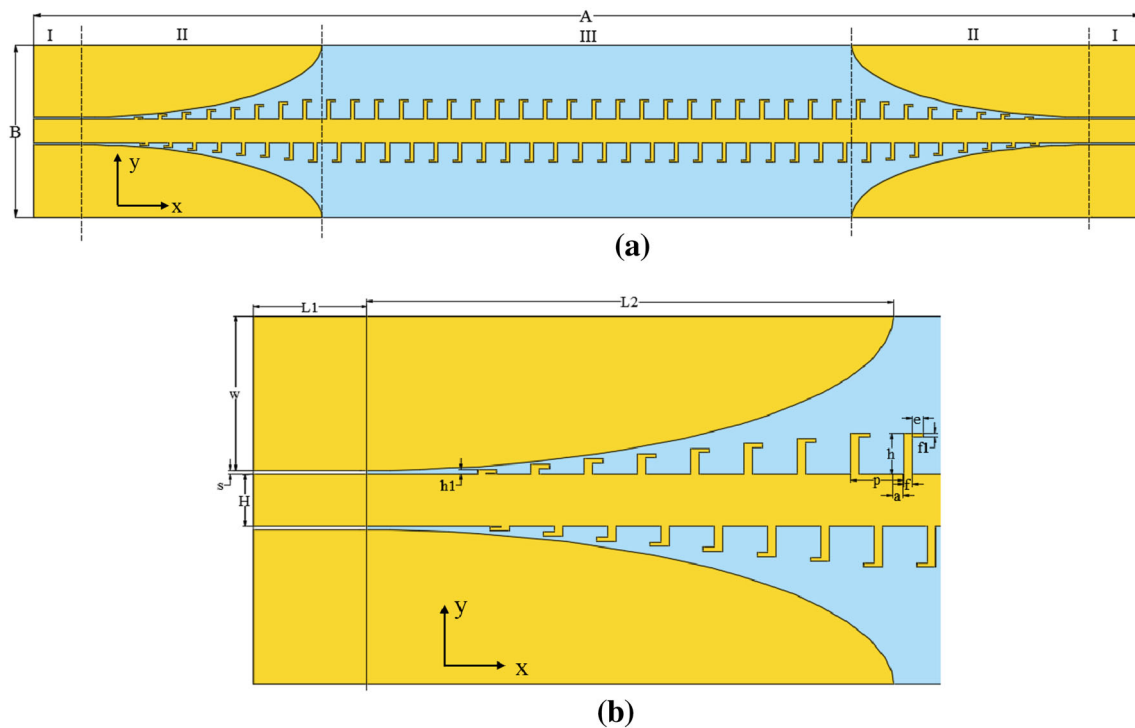

(a)

(b)

Fig. 2 a SSPP waveguide structure based on asymmetric serration units with b partial enlarged view of Regions I and II
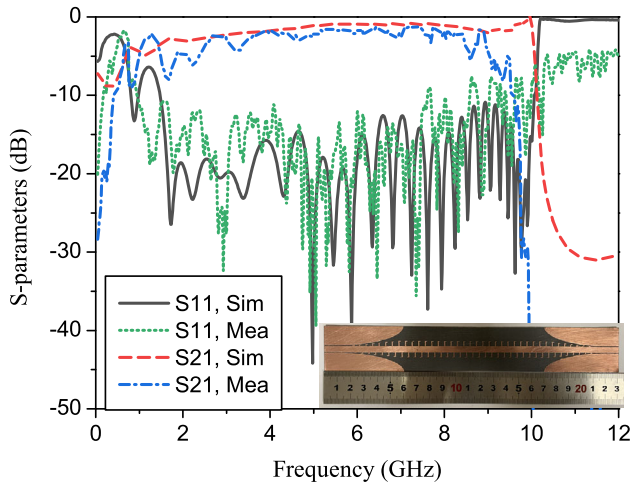
Fig. 3 The simulated and measured transmission characteristics of the constructed SSPP waveguide with e = 1.0 mm. The inset is the actual waveguide without the SMA connector soldered, and a ruler is attached to show its dimensions

deepening the groove. Therefore, the top conductor strip length e of the zigzag structure is used to regulate the passband range of the waveguide. The relationship between the dispersion characteristics and the conductor length e is shown in Fig. 4, where the zigzag conductor height is h = 4.0 mm and other structural parameters are determined according to Fig. 1a. It can be seen that with the increase of the length e, the asymptotic frequency of dispersion curve decreases significantly. In Fig. 1b, as the h value is changed from 3.0 to 4.0 mm, the cutoff frequency is reduced by 2.1 GHz. In Fig. 4, as the length e is increased from 0.0 to 3.0 mm, the cutoff
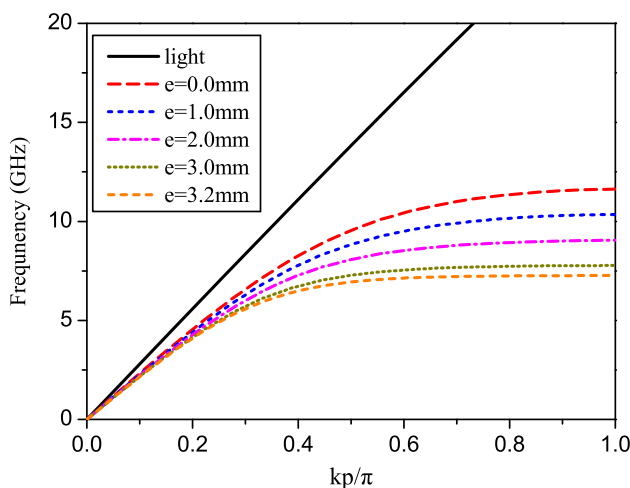
frequency is linearly reduced by 3.0 GHz, which cannot be achieved by adjusting the height h. As e = 3.2 mm, the cutoff frequency drops to 7.20 GHz.

The transmission characteristics of the SSPP waveguide with different e values are shown in Fig. 5. We can find that when the top conductor length e changes within 0.0–3.1 mm, the cutoff frequency changes significantly. The S_{21} value in the in-band is unchanged. This confirms that the waveguide passband can be well regulated using the top conductors. However, when the e value is greater than 3.2 mm, the in-band characteristics are significantly deteriorated to S_{21} less than − 6 dB. Although in that case the cutoff frequency is still reduced. It can be considered that e = 3.2 mm is the maximum limit for the waveguide band regulation. The cutoff frequencies for different e values shown in Fig. 5 are basically close to the asymptotic frequencies of the corresponding dispersion curves shown in Fig. 4. In the case of e = 0.0 mm, the cutoff frequency is 11.3 GHz. Thus, the regulation range of the cutoff frequency for the proposed SSPP waveguide is 7.2–11.3 GHz.

To experimentally verify the regulation effect of the top conductors on the waveguide transmission, two SSPP waveguides with e = 0.0 and 2.0 mm are also manufactured. The measured S-parameters of three waveguides with e = 0.0, 1.0, and 2.0 mm are shown in Fig. 6. We can clearly see that the cutoff frequency of the waveguide decreases with the increase of e value, while the low-frequency characteristics remain almost unchanged. Taking S_{21} greater than − 5 dB as the reference value, we can find that
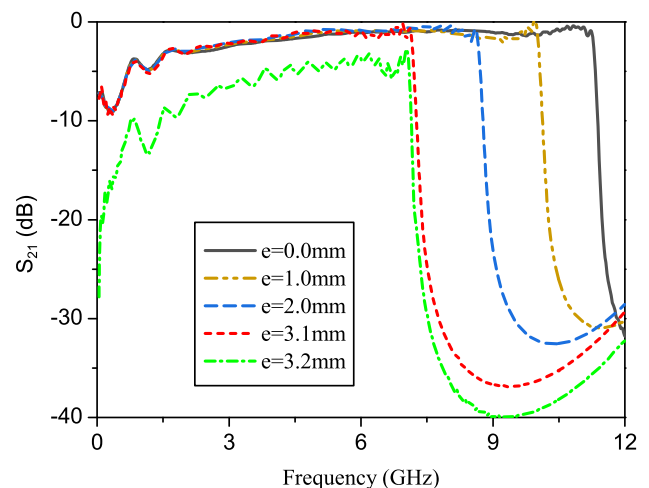

Fig. 4 Effect of the top conductor length e on the dispersion characteristics of the proposed asymmetric periodical unit

Fig. 5 Regulation of the top conductor length e on the transmission characteristics of the SSPP waveguide

as e = 0.0, 1.0, and 2.0 mm, the measured cutoff frequencies of the waveguide are 10.5, 9.4, and 8.5 GHz, respectively, which are a bit decreased compared to the simulation values.

4 Analysis and discussion

4.1 Comparison with symmetric periodic units

When the top conductor length of the serration unit shown in Fig. 1a is e = 0.0 mm, an asymmetric periodic unit similar to the traditional H-shaped structure is formed. The dispersion curves for the asymmetric unit without top lateral conductor and the traditional H-shaped unit are shown in Fig. 7. The two unit structures are exactly the same except for the different symmetry. We can see that the dispersion characteristics of two units are the same.

Furthermore, we add lateral conductor strips on top of the symmetrical H-shaped units to construct the SSPP waveguide with symmetric serration conductor periods. Figure 8 shows the transmission characteristics of the SSPP waveguide based on symmetric units with different lateral conductor lengths as other structural parameters are completely consistent with the waveguide shown in Fig. 2. We can see that with e = 2.2 mm, the transmission performance of the symmetric waveguide deteriorates significantly. The cuto ff frequency of the symmetric waveguide with e = 0.0 mm is 11.3 GHz, while that
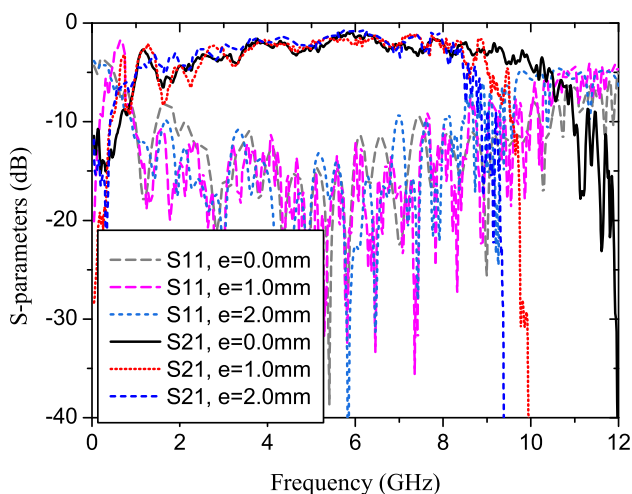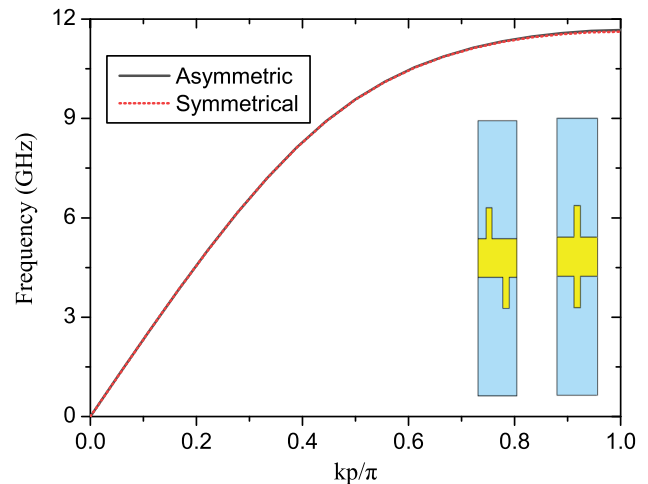

Fig. 7 The dispersion characteristics of symmetrical and asymmetrical periodic units

with e = 2.2 mm is 8.5 GHz. Thus, the adjustable range of the cutoff frequency for the symmetric waveguide is 8.5–11.3 GHz, which is smaller than that for the asymmetric structure. Moreover, a sag band appears on the high-frequency side of the passband, which is essentially an edge band with negative group velocity effect, and the steepness at the cutoff frequency becomes worse. This shows that, for a symmetric structure waveguide, the variation range of the cutoff frequency adjusted by the length of the lateral conductors is smaller than that of a waveguide based on asymmetric units.
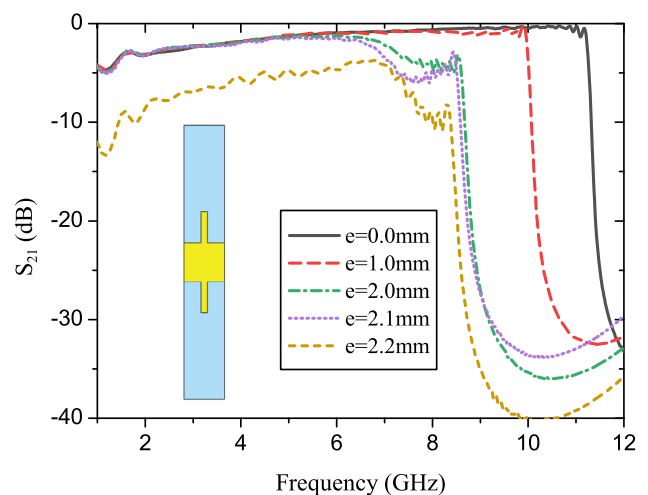

Fig. 6 Measured scattering parameters of three SSPP waveguides with e = 0.0, 1.0, and 2.0 mm

Fig. 8 The effect of the lateral conductor length e at the tops on the transmission characteristics of the waveguide with symmetric units

4.2 Field distribution characteristics

The SSPP waveguide has a stronger confinement field when it operates near the asymptotic frequency. The electric field component E_z on the xoy plane 0.5 mm away from the waveguide surface at 8.0 GHz is shown in Fig. 9, where the lateral conductor lengths of the asymmetric units are e = 0.0, 1.0, 2.0, and 3.2 mm, respectively. In that case, the excitation port is on the left side of the waveguide, and the right port is connected to the matched load. We can see that with e = 0.0, 1.0, 2.0 mm, the mode fields are effectively bound near the conductor surface, and the bound fields are the strongest in the case of e = 2.0 mm. As the top conductor length e increases, the single periodic area of the field distribution becomes smaller, which is equivalent to the enhancement of the wavelength shortening effect. However, with e = 3.2 mm, the periodic structures begin to lose the binding effect on SSPP modes. This also shows that the binding effect of the SSPP fields is mainly determined by the groove depth. However, as the depth exceeds a certain value, the low-frequency wave of the wavelength corresponding to the depth cannot form resonance in the narrow groove with a small width. Thus, the effective confinement of the fields cannot be achieved, and the guiding wave effect of SSPPs is weakened instead.

The intensity of the component E_z on the yoz plane of x = 115.0 mm at 8.0 GHz is shown in Fig. 10. As the lateral conductor length e increases, the electric field maximum value near the conductor surface clearly enlarges, indicating that the confinement of the waveguide to SSPP modes does increase with lengthening of the top conductor.

According to the multi-relaxation Lorentz model, the surface plasmon oscillation can be regarded as the coherent superposition of the oscillations of each unit, which leads to the strengthening of the oscillation [31]. From the viewpoint of an equivalent circuit, two adjacent periodic units form a resonance circuit with the resonant frequency $\omega = 1/\sqrt{LC}$, and the coupling between the resonance circuits realizes the transmission of SSPP modes [32–34]. As the top conductor length e increases, the equivalent inductance L increases. Since the gap between the lateral conductor and the adjacent unit decreases in this case, the equivalent capacitance C also increases. Therefore, the resonance frequency ω is reduced, and the electromagnetic energy is transmitted through the resonance mode coupling at a lower cutoff frequency. However, further increasing e value (for example, e = 3.2 mm), the resonance field area is no longer matched to the periodic structure unit. That is, the resonance wavelength is much greater than the structure period, so the SSPP mode transmission is no longer possible.
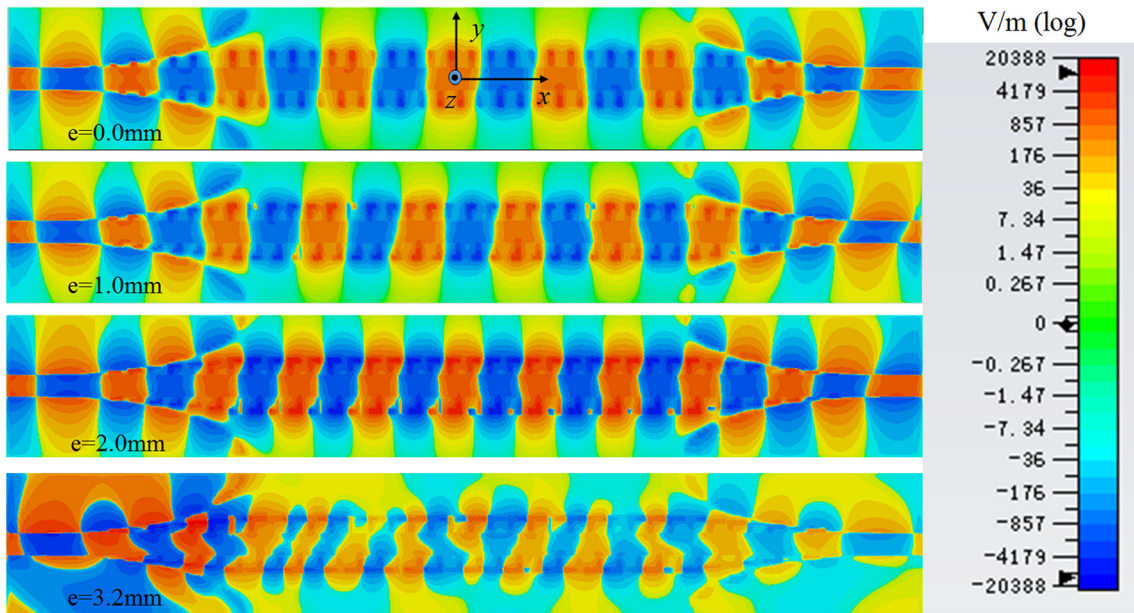

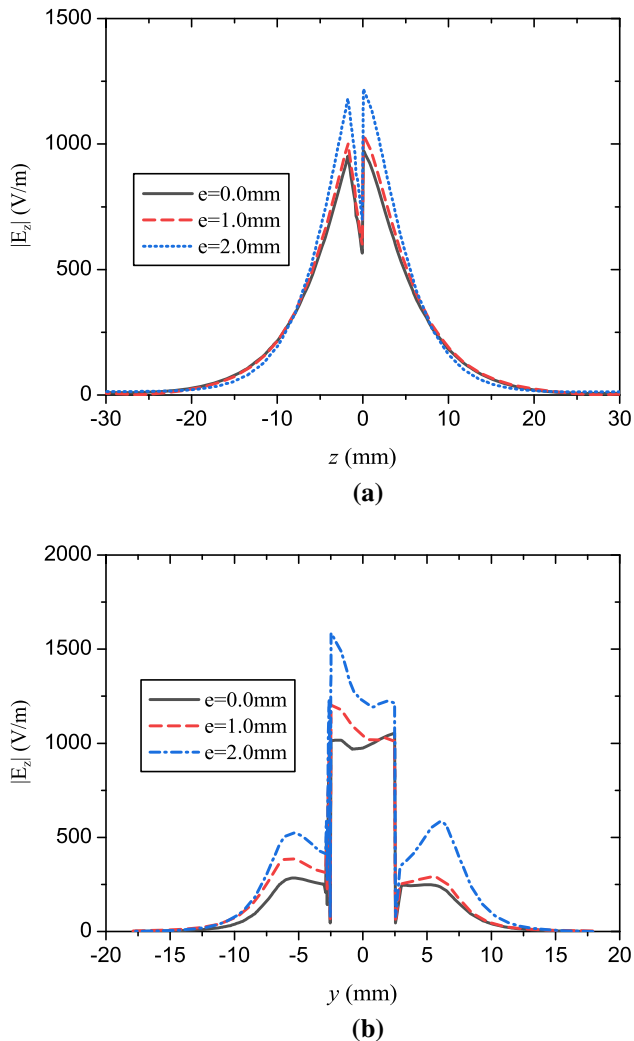**Fig. 9** The electric field component E_z on a plane 0.5 mm away from the SSPP waveguide surface at 8.0 GHz

Fig. 10 The z-direction electric field intensity variation at $x = 115.0$ mm at 8.0 GHz: **a** along the z axis, and **b** along the y axis

5 Conclusions

At the same frequency, the SSPP mode in the waveguide of a lower cutoff frequency has a more concentrated field distribution. For the SSPP waveguide with asymmetric serration structure units, it is verified that by loading lateral conductor strips on the serration tops, the confinement ability to SSPP surface waves can be improved without increasing the overall width of the waveguide conductor. In this case, the cutoff frequency is also reduced. By changing the length of the lateral conductor, an effective regulation of the cutoff frequency for the SSPP waveguide is achieved. Compared with the use of symmetric periodic units, this SSPP waveguide with

asymmetric serration unit structures can achieve wider passband adjustment to facilitate the construction of multifunctional SSPP devices.

Author contributions

All authors have the same contribute to the manuscript.

Data availability

The data that support the findings of this study are available from the corresponding authors upon reasonable request.

Declarations

Conflict of interest The authors declare that they have no conflict of interest.

References

1. W.L. Barnes, Surface plasmon–polariton length scales: a route to sub-wavelength optics. J. Opt. A **8**, S87 (2006)
2. C.R. Williams, S.R. Andrews, S.A. Maier, A.I. Fernandez-Dominguez, L. Martinmoreno, F.J. Garcia-Vidal, Highly confined guiding of terahertz surface plasmon polaritons on structured metal surfaces. Nat. Photonics **2**, 175 (2008)
3. F.J. Garcia-Vidal, L. Martin-Moreno, J.B. Pendry, Surfaces with holes in them: new plasmonic metamaterials. J. Opt. A **7**, S97 (2005)
4. J.B. Pendry, L. Martin-Moreno, F.J. Garcia-Vidal, Mimicking surface plasmons with structured surfaces. Science **305**, 847 (2004)
5. Y. Chen, Z. Song, Y. Li, M. Hu, Q. Xing, Z. Zhang, L. Chai, C.Y. Wang, Effective surface plasmon polaritons on the metal

wire with arrays of subwavelength grooves. Opt. Express **14**, 13021 (2006)

6. Q. Gan, Z. Fu, Y.J. Ding, F.J. Bartoli, Ultrawide-bandwidth slow-light system based on THz plasmonic graded metallic grating structures. Phys. Rev. Lett. **100**, 256803 (2008)

7. A. Rusina, M. Durach, M.I. Stockman, Theory of spoof plasmons in real metals. Appl. Phys. A **100**, 375 (2010)

8. X. Shen, T.J. Cui, D. Martin-Cano, F.J. Garcia-Vidal, Conformal surface plasmons propagating on ultrathin and flexible films. Proc. Natl Acad. Sci. USA **110**, 40 (2013)

9. H.C. Zhang, Q. Zhang, J.F. Liu, W. Tang, Y. Fan, T.J. Cui, Smaller-loss planar SPP transmission line than conventional microstrip in microwave frequencies. Sci. Rep. **6**, 23396 (2016)

10. H.C. Zhang, T.J. Cui, Q. Zhang, Y. Fan, X. Fu, Breaking the challenge of signal integrity using time-domain spoof surface plasmon polaritons. ACS Photonics **2**, 1333 (2015)

11. A.P. Hibbins, B.R. Evans, J.R. Sambles, Experimental verification of designer surface plasmons. Science **308**, 670 (2005)

12. Y.J. Zhou, Q.X. Xiao, Electronically controlled rejections of spoof surface plasmons polaritons. J. Appl. Phys. **121**, 123109 (2017)

13. H.C. Zhang, T.J. Cui, J. Xu, W. Tang, J.F. Liu, Real-time controls of designer surface plasmon polaritons using programmable plasmonic metamaterial. Adv. Mater. Technol. **2**, 1600202 (2017)

14. J. Xu, H.C. Zhang, W. Tang, J. Guo, C. Qian, W. Li, Transmission-spectrum-controllable spoof surface plasmon polaritons using tunable metamaterial particles. Appl. Phys. Lett. **108**, 191906 (2016)

15. X. Liu, Y. Feng, K. Chen, B. Zhu, J. Zhao, T. Jiang, Planar surface plasmonic waveguide devices based on symmetric corrugated thin film structures. Opt. Express **22**, 20107 (2014)

16. J.Y. Yin, J. Ren, H.C. Zhang, B.C. Pan, T.J. Cui, Broadband frequency-selective spoof surface plasmon polaritons on ultrathin metallic structure. Sci. Rep. **5**, 8165 (2015)

17. B.C. Pan, J. Zhao, Z. Liao, H.C. Zhang, T.J. Cui, Multi-layer topological transmissions of spoof surface plasmon polaritons. Sci. Rep. **6**, 22702 (2016)

18. Q. Zhang, H.C. Zhang, H. Wu, T.J. Cui, A hybrid circuit for spoof surface plasmons and spatial waveguide modes to reach controllable band-pass filters. Sci. Rep. **5**, 16531 (2015)

19. X. Gao, J. Shi, H.F. Ma, W.X. Jiang, T.J. Cui, Dual-band spoof surface plasmon polaritons based on composite-periodic gratings. J. Phys. D **45**, 505104 (2012)

20. X. Shen, T.J. Cui, Planar plasmonic metamaterial on a thin film with nearly zero thickness. Appl. Phys. Lett. **102**, 211909 (2013)

21. H. Xiang, Y. Meng, Q. Zhang, F.F. Qin, J.J. Xiao, D. Han, W. Wen, Spoof surface plasmon polaritons on ultrathin metal strips with tapered grooves. Opt. Commun. **356**, 59 (2015)

22. Y. Yang, X. Shen, P. Zhao, H.C. Zhang, T.J. Cui, Trapping surface plasmon polaritons on ultrathin corrugated metallic strips in microwave frequencies. Opt. Express **23**, 7031 (2015)

23. Y.Y. Yang, P. Gong, W.D. Ma, R. Hao, X.Y. Fang, Effects of substitution of group-V atoms for carbon or silicon atoms on optical properties of silicon carbide nanotubes. Chin. Phys. B **30**, 067803 (2021)

24. H.F. Ma, X. Shen, Q. Cheng, W.X. Jiang, T.J. Cui, Broadband and high-efficiency conversion from guided waves to spoof surface plasmon polaritons. Laser Photonics Rev. **8**, 146 (2014)

25. L. Ye, Y. Xiao, Y. Liu, L. Zhang, G. Cai, Q.H. Liu, Strongly confined spoof surface plasmon polaritons waveguiding enabled by planar staggered plasmonic waveguides. Sci. Rep. **6**, 38528 (2016)

26. X. Gao, L. Zhou, Z. Liao, H.F. Ma, T.J. Cui, An ultra-wideband surface plasmonic filter in microwave frequency. Appl. Phys. Lett. **104**, 191603 (2014)

27. Z. Liao, J. Zhao, B.C. Pan, X.P. Shen, T.J. Cui, Broadband transition between microstrip line and conformal surface plasmon waveguide. J. Phys. D **47**, 315103 (2014)

28. A. Kianinejad, Z.N. Chen, C. Qiu, Design and modeling of spoof surface plasmon modes-based microwave slow-wave transmission line. IEEE Trans. Microw. Theory Tech. **63**, 1817 (2015)

29. X. Wan, J.Y. Yin, H.C. Zhang, T.J. Cui, Dynamic excitation of spoof surface plasmon polaritons. Appl. Phys. Lett. **105**, 083502 (2014)

30. W. Li, Z. Qin, Y. Wang, L. Ye, Y. Liu, Spoof surface plasmonic waveguide and its band-rejection filter based on H-shaped slot units. J. Phys. D **52**, 365303 (2019)

31. Y.H. Jia, P. Gong, S.L. Li, W.D. Ma, X.Y. Fang, Y.Y. Yang, M.S. Cao, Effects of hydroxyl groups and hydrogen passivation on the structure, electrical and optical properties of silicon carbide nanowires. Phys. Lett. A **384**, 126106 (2020)

32. X. Tang, Q. Zhang, S. Hu, A. Kandwal, T. Guo, Y. Chen, Capacitor-loaded spoof surface plasmon for flexible dispersion control and high-selectivity filtering. IEEE Microw. Wirel. Compon. Lett. **27**, 806 (2017)

33. M.A. Kats, D. Woolf, R. Blanchard, N. Yu, F. Capasso, Spoof plasmon analogue of metal–insulator–metal waveguides. Opt. Express **19**, 14860 (2011)

34. R.K. Jaiswal, N. Pandit, N.P. Pathak, Center frequency and bandwidth reconfigurable spoof surface plasmonic metamaterial band-pass filter. Plasmonics **14**, 1539 (2019)